厚生労働科学研究費補助金（循環器疾患等総合事業）
分担研究報告書
弓部大動脈全置換術における超低体温療法と中等度低体温療法における血小板機能の比較検討

分担研究者　宮田茂樹　国立循環器病センター輸血管理室医長

研究要旨：従来までの超低体温を用いた弓部全置換術に比較して、生理的条件に近付けた 28℃中等度低体温下手術では、（超）低体温の弊害である体外循環時間の延長、臓器の温度較差、非生理的環境、それに基づく全身浮腫、肺障害、出血傾向などが回避でき、早期回復や出血が少ないなど「warm surgery」の利点が期待できうる。本研究では、中等度低体温下弓部全置換術と超低体温下弓部全置換術、それぞれの手術における血小板数、血小板機能を測定し、術中輸血量との関連を含めた解析を行うことにより、低体温の血小板機能、凝固関連因子に与えるインパクトを検討した。

　血小板機能の測定系として、平行板型フローチャンバーを用いたずり応力下血小板機能評価法を用い、低体温が血小板機能に与える影響について検討するとともに、術直前の血小板数、人工心肺中の最低血小板数ならびに術中総輸血量を低体温と中等度低体温で比較検討した。結果として、超低体温を用いて弓部全置換術を行った患者で、現時点で解析可能であった 6 症例における測定開始 5 分後の血小板血栓の高さは、人工心肺離脱直後（血小板輸血実施前）では 4.46 ± 0.63 μm (n=6)あった。一方、中等度低体温を用いて弓部全置換術を行った患者で、現時点で解析可能であった 2 症例における人工心肺離脱直後（血小板輸血実施前）の測定開始 5 分後の血小板血栓の高さは 4.9 ± 0.42　μm (n=2)で、中等度低体温患者の方が、超低体温を用いた患者より人工心肺離脱直後（血小板輸血実施前）のずり応力下血小板血栓形成能が若干高い傾向が認められた。また、中等度低体温弓部全置換術において、超低体温を用いた弓部全置換術と比較して、人工心肺中最低血小板数が高い傾向にあり、さらに、これらの結果に合致して、赤血球製剤、新鮮凍結血漿、濃厚血小板製剤の輸血量が、少ない傾向が認められた。

　現時点で、登録された患者数が少なく、解析可能な患者数が限られているため、明確ではないが、中等度低体温では、人工心肺中の血小板に対する環境として、超低体温より有利に働き、血小板数ならびに血小板機能が保護され、出血量が少なく、止血効果が良好となる可能性があることが示唆された。

A. 研究目的

　近年、高齢化が進み、大動脈疾患に対する手術件数は冠動脈手術と共に増加の一途をたどっている。しかしながら、通常の開心術に比べ、高い手術侵襲度、手術の困難さ、患者の高齢化、多岐にわたる併存疾患、大量出血などの問題があり、その手術成績の向上は急務である。特に、弓部大動脈瘤に対する人工血管置換術（弓部全置換術）はその中心をなし、生命予後に止まらず、高次機能を含め脳保護法は未だに重要な課題である。我が国では、脳保護法として、従来からの超低体温循環停止に加え、補助手段として選択的順行性脳灌流（SCP）と逆行性脳灌流（RCP）が開発され臨床応用されてきた。最近では、時間的制約の少ない点から、より生理的な SCP が定着し広く用いられている。この SCP を用いた場合、脳の灌流が維持されており、必ずしも超低体温を用いる必要がない。その観点から、最近になり生理的条件に近付けた 28℃中等度低体温下手術が試みられ、有効性が報告されつつある。弓部全置換術においても、通常の開心術の進歩、発展と同様に、（超）低体温の弊害である体外循環時間の延長、臓器の温度較差、非生理的環境、それに基づく全身浮腫、肺障害、出血傾向などが回避でき、早期回復や出血が少ないなど「warm surgery」の利点が期待できうる。しかしながら、前述の報告では、比較対照群がなく単独での報告であり、従来からの超低体温下弓部全置換と比べどの程度の有用性、安全

性があるかは明確にされていない。中等度低体温下手術の有効性を明らかにするためには、従来からの超低体温下弓部全置換との厳密な比較検討が必要とされる。本研究では、中等度低体温下弓部全置換術と超低体温下弓部全置換術における多施設共同前向き調査研究の一環として、中等度低体温下弓部全置換術と超低体温下弓部全置換術、それぞれの手術における血小板数、血小板機能を測定し、術中、術後の輸血量との関連を含めた解析を行うことにより、低体温の血小板機能、凝固関連因子に与えるインパクトを検討することとした。

弓部全置換術の場合、人工心肺を必要とすることで血小板機能低下が起こる事が指摘されている。また、血小板機能に体温が与える影響についても指摘されている。また、ヘパリン、プロタミンを使用する等で、血小板機能が損なわれるという報告も存在する。したがって、本研究では、血小板数だけでなく、血小板機能に関する評価を行った。近年、血小板機能を評価する場合に、生体内で血小板が存在する環境である流動状況下での血小板機能を考慮する必要性が指摘され、ずり応力下血小板機能評価の新しい概念が確立されつつある。生理的条件に近い系として、体温が血小板機能に与える影響を in vitro で、血小板膜レセプターと各種粘着蛋白との相互作用を含めた詳細な評価が可能となる。本研究では、ずり応力下血小板機能評価法を用い、低体温が血小板機能に与える影響について検討した。

B. 研究方法
1) ずり応力下血小板機能測定

術直前ならびに、人工心肺離脱直後（血小板輸血を実施する前）に、抗凝固剤として選択的抗トロンビン剤であるアルガトロバンを終濃度 125 μg/ml となるよう添加し採血した検体を用いて検討した。術直前もしくは人工心肺離脱直後（血小板輸血を実施する前）に採血した全血をコラーゲン Type I を固相化したガラスプレートを組み込んだ平行板型フローチャンバー内に、血小板を蛍光色素（メパクリン）で標識して流し込み、高ずり応力(2000/s)のかかる部位でのコラーゲン固相表面上での血小板血栓形成過程を倒立型蛍光顕微鏡でリアルタイムに観察した。また、これらの画像を CCD カメラによりコンピュータに取り込みデジタル化し、画像解析を行った。測定開始5分後に形成された血小板血栓をZ方向にスキャンすることにより血小板血栓の3次元イメージを再構築し、血小板血栓の高さを測定することにより血小板機能の指標とした。

2) 血小板数並びに術中輸血量

術直前の血小板数、人工心肺中の最低血小板数ならびに術中総輸血量を低体温と中等度低体温で比較検討した。

C. 研究結果
1) ずり応力下血小板機能測定

超低体温を用いて弓部全置換術を行った患者で、現時点で解析可能であった6症例における術前検体を平行板型フローチャンバー内に流し込み解析をおこなった。測定開始5分後の血小板血栓の高さは、18.4（平均）±4.2（1 S.D.）μm (n=6)であった。人工心肺離脱直後（血小板輸血実施前）の測定開始5分後の血小板血栓の高さは 4.46 ± 0.63 μm (n=6)であった。一方、中等度低体温を用いて弓部全置換術を行った患者で、現時点で解析可能であった2症例における術前の測定開始5分後の血小板血栓の高さは、19.9 ± 4.1 μm (n=2)、人工心肺離脱直後（血小板輸血実施前）では4.9 ± 0.42 μm (n=2)であった。現時点で、登録された患者数が少なく、解析可能な患者数が限られているため、明確ではないが、中等度低体温患者の方が、超低体温を用いた患者より人工心肺離脱直後（血小板輸血実施前）のずり応力下血小板血栓形成能が若干高い傾向が認められた。

2) 血小板数ならびに術中輸血量

超低体温を用いて弓部全置換術を行った患者で、現時点までに、登録された6症例における術前血小板数は、171,300（平均）± 31,600（1 S.D.）/μl,（n=6）、人工心肺中の最低血小板数は42,100±

16,700 /μl（n=6）あった。一方、中等度低体温を用いて弓部全置換術を行った患者で、現時点までに、登録された 3 症例における術前血小板数は、213,700 ± 49,100/μl,（n=3）、人工心肺中の最低血小板数は 65,700 ± 18,900 /μl（n=3）であった。

　超低体温を用いて弓部全置換術を行った患者で、現時点までに、登録された 6 症例における術中総輸血量は、赤血球製剤は、22.6 単位 ±14.2 単位、新鮮凍結血漿 28.0 単位 ± 19.2 単位、濃厚血小板製剤 41.4 単位 ±22.9 単位(n=6)であった。一方、中等度低体温を用いて弓部全置換術を行った患者で、現時点までに、登録された 3 症例における術中輸血量は、赤血球製剤 14.7 単位 ±12.9 単位、新鮮凍結血漿 15.3 単位 ± 13.6 単位、濃厚血小板製剤 10.0 単位 ±17.3 単位（n=3）であった。現時点で、登録された患者数が少なく、解析可能な患者数が限られているため、明確ではないが、中等度低体温患者の方が、超低体温を用いた患者より、人工心肺中最低血小板数が高値であり、術中輸血量（赤血球製剤、新鮮凍結血漿、濃厚血小板製剤のいずれにおいても）が少ない傾向が認められた。これは、人工心肺離脱直後のずり応力下血小板血栓形成能が若干高いという結果と、合致するものと思われた。

D. 考案

　従来までの超低体温を用いた弓部全置換術に比較して、生理的条件に近付けた 28℃中等度低体温下手術では、（超）低体温の弊害である体外循環時間の延長、臓器の温度較差、非生理的環境、それに基づく全身浮腫、肺障害、出血傾向などが回避でき、早期回復や出血が少ないなど「warm surgery」の利点が期待できうる。

　本研究では、中等度低体温下弓部全置換術と超低体温下弓部全置換術、それぞれの手術における血小板数、血小板機能を測定し、術中輸血量との関連を含めた解析を行うことにより、低体温の血小板機能、止血機能に与えるインパクトを検討した。結果として、中等度低体温弓部全置換術において、超低体温を用いた弓部全置換術と比較して、

術中血小板数ならびに血小板機能が良好である事が示唆された。また、これらの結果に合致して、赤血球製剤、新鮮凍結血漿、濃厚血小板製剤の輸血量が少ない傾向が認められた。

　中等度低体温では、人工心肺中の血小板に対する環境として、超低体温より有利に働き、血小板数ならびに血小板機能が保護され、出血量が少なく、止血効果が良好となる可能性があることが示唆された。現時点で、登録された患者数が少なく、解析可能な患者数が限られているため、明確ではないが、今後、症例を積み重ねさらに検討を続けていきたい。

E. 結論

● 中等度低体温では、人工心肺中の血小板に対する環境として、超低体温より有利に働き、血小板数ならびに血小板機能が保護され、出血量が少なく、止血効果が良好となる可能性があることが示唆された。

G. 関連する研究発表

1. 論文発表

1) Banno F, Kokame K, Okuda T, Honda S, Miyata S, Kato H, Tomiyama Y, Miyata T. Complete deficiency in ADAMTS13 is prothrombotic, but it alone is not sufficient to cause thrombotic thrombocytopenic purpura. Blood. in press.

2) Shiraga H., Miyata S., Kato H., Kashiwagi H., Honda S., Kurata Y., Tomiyama Y., Kanakura Y. Impaired platelet function in a patient with $P2Y_{12}$ deficiency caused by a mutation in the translation initiation codon. J Thrmb Haemost 2005; 3: 2315-2323.

3) Kato H., Kashiwagi H., Shiraga M., Tadokoro S, Kamae T., Ujiie H., Honda S., Miyata S., Ijiri Y., Yamamoto J., Maeda N., Funahashi T., Kurata Y., Shimomura I., Tomiyama Y., Kanakura Y. Adiponectin acts as an endogenous antithrombotic factor. Arterioscler Thromb Vasc Biol. 2006; 26: 224-230.

2. 学会発表

1) <u>Miyata S.</u>, Kamei M. Developing and implementing local guidelines for appropriate and safe clinical blood transfusion (based on actual experiences). WHO Workshop on Appropriate and Safe Clinical Blood Transfusion. Macao, China, 2005.

2) <u>Miyata S.</u>, Kamei M. Effective interventions in changing the prescribing habit of blood transfusion (based on local experiences). WHO Workshop on Appropriate and Safe Clinical Blood Transfusion. Macao, China, 2005.

3) 今林徹、亀井政孝、<u>宮田茂樹</u>、山本賢、河合健、佐野隆宏、八木原俊克、畔政和：ファロー四徴症修復術における人工心肺中最低ヘモグロビン値の術後30日間死亡率および合併症発症率に与える影響．第53回日本輸血学会総会、東京、2005．

4) 今林徹、亀井政孝、康雅博、<u>宮田茂樹</u>、山本賢、河合健、佐野隆宏、小林順二郎、畔政和：心拍動下冠動脈バイパス術症例では術前貯血式自己血貯血は無輸血率に影響しない．第53回日本輸血学会総会、東京、2005．

5) <u>宮田茂樹</u>：安全で適正な心臓血管外科周術期輸血管理についての検討、第58回日本胸部外科学会定期学術集会、岡山、2005

6) <u>宮田茂樹</u>：血小板保存期間と血小板機能．第29回日本血液事業学会．仙台、2005

7) <u>宮田茂樹</u>：緊急時対応を含んだ適正で安全な輸血療法を支援する輸血管理システムの運用．第33回日本救急医学会総会、埼玉、2005

8) <u>宮田茂樹</u>："使用指針"の限界－血液製剤ならびに血漿分画製剤－．第25回日本臨床麻酔学会総会、大阪、2005．

H. 知的財産権の出願・登録状況
なし

弓部大動脈全置換術における超低体温療法と中等度低体温療法のランダム化比較試験に
関する研究：弓部大動脈全置換術における超低体温療法の中等度低体温療法の多施設共同
前向き調査研究

荻 野　　均　　　　八 木 原　俊 克　　　　湊 谷　謙 司　　　松 田　　均
佐 々 木　啓 明　　　嘉 田　晃 子

研究要旨：従来の弓部大動脈全置換術は 20℃超低体温を基本としてきたが、最近になり、
安定した選択的順行性脳灌流下に、超低体温の弊害を考慮し徐々に最低温を上げる傾向に
ある。一部の施設では 28℃中等度低体温下手術が試みられ良好な成績が報告されつつある。
本研究においては、28℃中等度低体温下弓部全置換術と 20℃超（深度）低体温下弓部全置
換術における多施設共同前向き調査研究を行い、それぞれの弓部全置換術の特徴を明らか
にすることにある。

A. 研究目的

　12〜15℃前後の超低体温循環停止法を用いて
開始された弓部全置換術は、選択的順行性脳灌流
（SCP）や逆行性脳灌流（RCP）などの有用な脳
保護手段が開発され、それ以前の手術と比べ著し
い成績の向上をみた。しかしながら、共に 20℃以
下の超低体温を基本としており、超低体温の弊害
である体外循環の延長、臓器の温度格差、非生理
的条件、それに基づく全身浮腫、肺障害、出血傾
向などの不利な条件下に成立している。したがっ
て、対象患者の多くを 70 歳以上の高齢者が占め
る現状においては、このような超低体温法に基づ
く弊害は術後の回復遅延や手術成績の悪化につ
ながる可能性があり、更なる改良・改善が望まれ
ている。一方、生理的な脳灌流である SCP 下で
は必ずしも超低体温を用いる必要がないと考え
られ、したがって、最近では一部の施設において
28℃中等度低体温下弓部全置換術が試みられ、良
好な成績が報告されてきている。ところが、超低
体温下弓部全置換術と中等度低体温下弓部全置
換術を厳密に比較し、各々の手技の長所、短所を
明確にした報告はない。そのような現状から、本
研究は、まず、28℃中等度低体温下弓部全置換術
と 20℃超（深度）低体温下弓部全置換術における
多施設共同前向き調査研究を行い、それぞれの弓
部全置換術の特徴を明らかにすることにある。将
来的には、本研究で得られた利点のいくつかを主
要項目として設定し、より厳密に二群間でランダ
ム化比較試験を行い、中等度低体温下弓部全置換
術の優位性を明らかにすることを最終目的とし
ている。

B. 研究方法

　SCP を脳保護手段とした弓部全置換術にお
いて、28℃中等度低体温下弓部全置換術と 20℃
超低体温下弓部全置換術における多施設共同

前向き調査研究を行う。緊急患者、再手術患者を除いた待機的弓部全置換術患者を対象とする。手術は、胸骨正中切開下に体外循環を上行大動脈、腋窩動脈、大腿動脈送血、上・下大静脈ないしは右房脱血により確立する。SCP を脳保護手段として、4分枝人工血管を用いた弓部分枝個別再建法により弓部全置換を行う。各群の SCP 圧、SCP 量は以下のとおりとする。

① 膀胱温 20℃ SCP 圧 30-50 mmHg → 10 ml/kg/min が目安

② 膀胱温 28℃ SCP 圧 ≧50 mmHg → 15〜25 ml/kg/min が目安。

比較評価項目は、

1) 28℃中等度低体温下弓部全置換群と 20℃超低体温下弓部全置換群における術後 30 日以内死亡、および脳・脊髄障害、心臓障害、肺障害、腎障害、出血、感染、などの合併症の発生割合

2) 臨床データ： ① 手術時間など、② 出血量、輸血量など、 ③循環動態、 ④呼吸状態、⑤脳機能、⑥肝・腎機能、 ⑦ 血液凝固機能、 ⑧ 回復状況。

C. 研究結果

本年度は、国立循環器病センターで 2002 年以降に待機的弓部全置換術を行った患者 114 例について、20℃ 37 例、25℃ 44 例、28℃ 33 例の 3群に分け、術中データ、合併症を含めた成績についてレトロスペクティブに比較検討した。その結果、3群間で手術死亡、脳合併症の発生に差を認めず、28℃群で復温時間および心筋虚血時間の短縮が得られた。また、28℃群で、血小板使用頻度が少なく、ICU 帰室時の体温が高く、乳酸値が低い傾向が得られた。この結果を第 85 回アメリカ胸部外科学会で発表した。この結果を踏まえ、より詳細にデータを収集し厳密に比較検討すべく、今回の多施設共同前向き調査研究を企画した。目標症例数は 100 例を予定している。

D. 考察

アメリカ胸部外科学会で報告した内容から、28℃中等度低体温下手術の、出血面、術後早期回復面での限られた優位性が示唆されたが、レトロスペクティブ研究であり、綿密なデータの収集が行えておらず、統計上、明らかな有意性を持って評価できる項目が検出できなかった。したがって、多施設共同前向き調査研究の形をとって、綿密にデータを収集し、28℃中等度下手術と 20℃超低体温下手術の特徴を明らかにすることから開始した。

28℃中等度低体温下手術の優位性は、出血量の少なさ、早期回復などにあると予想されるが、一方で、安定した SCP 下であるとは言え、温度が上昇すれば、脳保護の面で 20℃超低体温下手術と異なる部分が生じる。28℃下ではより高流量の SCP が必要なことが予想されるが、未だ十分な検討がなされていない。その面で、本研究では MRI 検査および高次機能検査などの脳機能検査が組み込まれており、脳保護の面で 28℃中等度低体温下手術の特徴、安全性が明らかになるものと期待される。本研究の最終目的は、症例を厳密に選択した条件下での 28℃中等度低体温下手術と 20℃超低体温下手術とのランダム化比較試験であり、本研究から得られた適切な評価項目をエンドポイントとして設定し、ランダム化比較試験につなげる予定である。

E. 結論

未だ症例登録中であり、結論は来年度に持ち越しである。本研究は臨床的に妥当で、今後も遂行可能と考える。

F. 健康危険情報

特になし。

G. 研究発表

1. 学会発表

1) Minatoya K, Ogino H, Matsuda H, Sasaki H, Yagihara T, Kitamura S. Evolving selective cerebral perfusion for aortic arch

operations: high flow rate with moderate
hypothermic circulatory arrest. 85th AATS
San Francisco, CA, 2005.4.11

2. 論文発表

1) Ogino H, Ando M, Sasaki H, Minatoya
   K. Total arch replacement using a stepwise
   distal anastomosis for arch aneurysms with
   distal extension. European Journal of
   Cardiothoracic Surgery. 2006

2) Minatoya K, Ogino H, Matsuda H, Sasaki
   H, Yagihara T, Kitamura S. Surgical
   management of distal arch aneurysm:
   another approach with improved results.
   Ann Thorac Surg. 2006

H. 知的財産権の出願登録状況
本研究課題に関連する当該事項の登録はない。

III. 研究成果の刊行物・別刷

How-to-do-it

Total arch replacement using a stepwise distal anastomosis for arch aneurysms with distal extension[☆]

Hitoshi Ogino [a,*], Motomi Ando [b], Hiroaki Sasaki [a], Kenji Minatoya [a]

[a] *Department of Cardiovascular Surgery, National Cardiovascular Center, 5-7-1 Fujishirodai, Suita, Osaka 565-8565, Japan*
[b] *Department of Thoracic Surgery, Fujita Health University, Mizukake-cho, Toyoake, Aichi 470-1192, Japan*

Abstract

A total of 120 patients having arch to distal arch aneurysm with downstream extension underwent total arch replacement, with individual arch-vessel reconstruction through median sternotomy using a novel 'stepwise' distal aortic anastomosis. Cardiopulmonary bypass was established by cannulating the right axillary artery and the ascending aorta or femoral artery. Hypothermia was at 22–28 °C. Through the aneurysm, the descending aorta was divided. Distal anastomosis using the stepwise technique was performed; a tube graft of length 7–12 cm was inserted into the descending aorta and anastomosed by running suture. The distal end of the inserted graft was extracted, and a further four-branched arch graft was joined to it. Selective cerebral perfusion was used for cerebral safety during arch repair. There were three hospital deaths (2.5%). Two patients (1.7%) developed permanent neurological dysfunction and three patients (2.5%) suffered transient cerebral deficits. Three patients (2.5%) required reentry for postoperative bleeding although in none of them bleeding was from the distal anastomosis site with the stepwise technique. Stepwise anastomosis is a useful and secure alternative for distal anastomosis in total arch replacement for arch to distal arch aneurysms with distal extension.
© 2005 Elsevier B.V. All rights reserved.

Keywords: Aortic arch; Aneurysm; Aortic dissection; Aortic surgery

1. Introduction

For arch to distal arch aneurysms, it is not agreed whether a median or lateral approach is better, particularly for aneurysms with distal extension [1–7]. The median approach aims to provide cerebral and cardiac safety [1–4]. However, the distal anastomosis is often difficult and bleeding from it is a serious problem [6,7]. We have therefore used a novel stepwise technique providing a technically easy and secure anastomosis.

2. Patients and methods

Between 1999 and 2003, 120 patients (74 years old) having an arch to distal arch aneurysm underwent total arch replacement. Of these, 112 patients had non-dissecting and two had dissecting aneurysms. The other six had a combined pathology. Ten patients required emergency surgery.

The aneurysm was approached through median sternotomy (Fig. 1A). After full heparinization, a 10–16 Fr straight

thin-wall cannula was inserted into the right axillary artery (RAxA) on the right armpit [8]. Cardiopulmonary bypass (CPB) was established by cannulation involving also the femoral artery or the ascending aorta. The patients were cooled to 22–28 °C. Following hypothermic circulatory arrest, selective cerebral perfusion (SCP) was begun through the RAxA perfusion by clamping the brachiocephalic artery (BCA). The arch was opened and a 12 Fr SCP balloon cannula was inserted into the left common carotid artery (LCCA) (Fig. 1B). In recent series with moderate hypothermia at 25–28 °C, the left subclavian artery (LSCA) was also perfused. With SCP, the descending aorta was divided through the aneurysm. Distal aortic anastomosis was done using a stepwise technique. First, an invaginated tube graft of length 7–12 cm (a piece of the quadrifurcated arch graft) was inserted into the descending aorta (Fig. 1C). The position of the proximal end of the invaginated graft was adjusted to match the level of the divided end of the descending aorta. The anastomosis was then easy to perform, with a good surgical view, using an over and over running suture of 3-0 or 4-0 polypropylene, with reinforcement by Teflon felt strip (Fig. 2A). The distal end of the inserted graft was extracted proximally. For arch reconstruction, a further four-branched arch graft was attached to this stepwise graft using a running 3-0 polypropylene suture (Fig. 2B). Antegrade aortic perfusion was initiated. The LSCA was reconstructed with a branch graft.
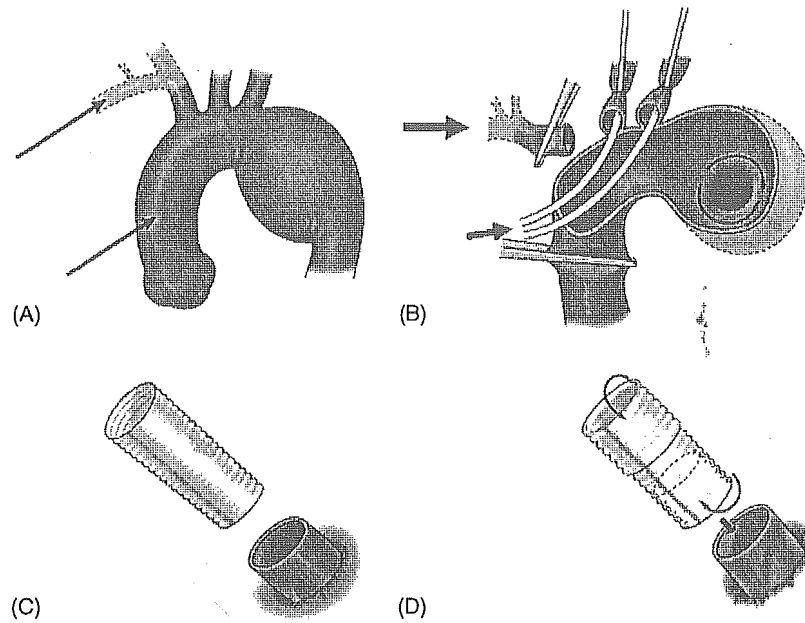
Fig. 1. Total arch replacement using selective cerebral perfusion and stepwise distal anastomosis. (A) Distal arch aneurysm: black arrows show cannulation sites on the right axillary artery and the ascending aorta for cardiopulmonary bypass. (B) Brain protection with antegrade selective cerebral perfusion (SCP): large (right axillary artery perfusion) and small (left common carotid and left subclavian artery perfusion) arrows show SCP. The descending aorta was divided from the inside through the aneurysm. (C) An invaginated tube graft was inserted into the descending aorta. (D) Recent refined technique (mini-elephant trunk technique): 2–3 cm of the proximal end was left without invagination so as to reinforce the anastomosis from the inside by a 'sandwich' technique with the outside Teflon felt strip. The distal end was also tucked inside to shorten the length of the graft, in order to prevent dislodge of the mural atheroma.

Rewarming was then initiated. The proximal anastomosis was done above the sinotubular junction. Finally, the LCCA and the BCA were reconstructed (Fig. 2C). The RAxA perfusion was discontinued. In recent cases, our stepwise technique was refined to reinforce the anastomosis and prevent bleeding from the anastomosis (Fig. 1D). In making the stepwise graft, 2–3 cm of the proximal end was left without invagination so as to reinforce the anastomosis from the inside by a 'sandwich' technique with the Teflon felt strip. We call this 'mini-elephant trunk technique'. Coronary artery bypasses grafting in 23, aortic valve replacement in one, and mitral valve plasty in one were also performed.
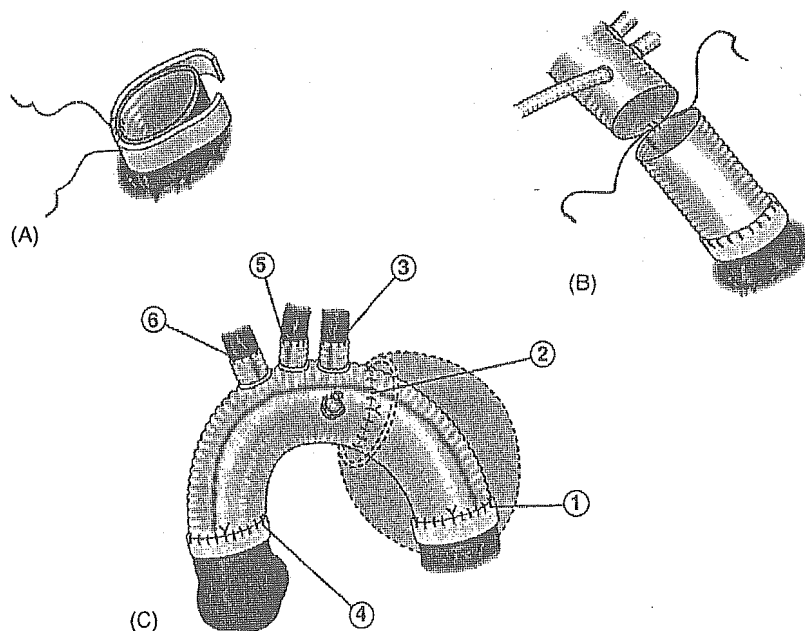

Fig. 2. Stepwise distal anastomosis. (A) Stepwise distal anastomosis with the reinforcement of outside Teflon felt strip using a running suture. (B) The distal end of the inserted graft was extracted and a quadrifurcated arch graft was connected to this end. (C) Total arch replacement using a stepwise anastomosis: the numbers show the turn of anastomosis.

3. Results

The median duration of lower body circulatory arrest, SCP, CPB, and surgery were 68, 147, 209, and 415 min, respectively. The median transfusion volume was 2400 ml. There were three hospital deaths (2.5%) from perioperative myocardial infarction, low cardiac output with bowel necrosis, and mediastinitis. Two patients (1.7%) developed permanent neurological dysfunction (small stroke), and three patients (2.5%) suffered from transient cerebral deficits. Three patients (2.5%) required reentry for bleeding. In none of them, bleeding from the distal anastomosis was found. Other complications occurred: low cardiac output in 5.0%, respiratory failure in 10.0%, renal failure in 3.3%, hepatic failure in 0.8%, bowel necrosis in 1.7%, and sepsis in 0.8%.

4. Discussion

The most common approach for arch to distal arch aneurysms is currently through median sternotomy [1–4]. This approach aims to provide cerebral and cardiac safety. However, the distal anastomosis tends to be difficult because of poor, distant, and limited view [6,7]. In our technique, the arch aneurysm is not incised to prevent injury to the nerves and lung. Through the aneurysm, the descending aorta is divided and the distal anastomosis takes place. Subsequently, the surgical view is limited. Furthermore, bleeding from this anastomosis is a major concern. We have therefore evolved a novel stepwise technique, which made the distal anastomosis around the hilum feasible in our experience.

The end of the descending aorta is often fragile with much atherosclerosis. Even with the stepwise technique, we experienced bleeding from the anastomosis in seven patients. The stepwise technique was therefore refined by the "mini-elephant trunk". With this refinement, we have not experienced any major bleeding from the distal anastomosis.

The stepwise technique has some drawbacks. Graft insertion carries a risk of dislodging mural atheroma. We experienced one case of bowel necrosis. To prevent this problem, in the refined technique, the distal end was tucked inside to shorten the graft length. Graft insertion must be done carefully into the atheromatous descending aorta. Direct anastomosis of a short-length graft without graft insertion is a good alternative. Another disadvantage is the need for a graft–graft anastomosis, which is fortunately easy with a good view taking 5–10 min.

References

[1] Bachet J, Guilmet D, Goudot B, Dreyfus GD, Delentdecker P, Brodaty D, Dubois C. Antegrade cerebral perfusion with cold blood: a 13-year experience. Ann Thorac Surg 1999;67:1874–8.

[2] Kazui T, Washiyama N, Muhammad BA, Terada H, Yamashita K, Takinami M. Total arch replacement using aortic arch branched grafts with the aid of antegrade selective cerebral perfusion. Ann Thorac Surg 2000;70(1):3–8.

[3] Kazui T, Washiyama N, Muhammad BA, Terada H, Yamashita K, Takinami M. Improved results of atherosclerotic arch aneurysm operations with a refined technique. J Thorac Cardiovasc Surg 2001;121(3):491–9.

[4] Kazui T, Yamashita K, Washiyama N, Terada H, Bashar AH, Suzuki T, Ohkura K. Usefulness of antegrade selective cerebral perfusion during aortic arch operations. Ann Thorac Surg 2002;74(5):S1806–9.

[5] Takamoto S, Okita Y, Ando M, Morota T, Handa N, Kawashima Y. Retrograde cerebral circulation for distal aortic arch surgery through a left thoracotomy. J Card Surg 1994;9(5):576–82 [discussion 582–3].

[6] Ogino H, Ueda Y, Sugita T, Matsuyama K, Matsubayashi K, Nomoto T, Yoshioka T. Aortic arch repairs through three different approaches. Eur J Cardiothorac Surg 2001;19(1):25–9.

[7] Westaby S, Katsumata T. Proximal aortic perfusion for complex arch and descending aortic disease. J Thorac Cardiovasc Surg 1998;115:162–7.

[8] Numata S, Ogino H, Sasaki H, Hanafusa Y, Hirata M, Ando M, Kitamura S. Total arch replacement using antegrade selective cerebral perfusion with right axillary artery perfusion. Eur J Cardiothorac Surg 2003;23(5):771–5.

ORIGINAL ARTICLE

Impaired platelet function in a patient with P2Y$_{12}$ deficiency caused by a mutation in the translation initiation codon

M. SHIRAGA,* S. MIYATA,† H. KATO,* H. KASHIWAGI,* S. HONDA,* Y. KURATA,‡ Y. TOMIYAMA* and Y. KANAKURA*

Department of Hematology and Oncology, Graduate School of Medicine C9, Osaka University, Osaka, Japan; †Division of Blood Transfusion Medicine, National Cardiovascular Center, Osaka, Japan; and ‡Department of Blood Transfusion, Osaka University Hospital, Osaka, Japan

Summary. In this study, we have identified a patient (OSP-1) with a congenital P2Y$_{12}$ deficiency showing a mild bleeding tendency from her childhood and examined the role of P2Y$_{12}$ in platelet function. At low concentrations of agonists OSP-1 platelets showed an impaired aggregation to several kinds of stimuli, whereas at high concentrations they showed a specifically impaired platelet aggregation to adenosine diphosphate (ADP). ADP normally induced platelet shape change and failed to inhibit PGE$_1$-stimulated cAMP accumulation in OSP-1 platelets. Molecular genetic analysis revealed that OSP-1 was a homozygous for a mutation in the translation initiation codon (A$\underline{T}$G to A$\underline{G}$G) in the *P2Y$_{12}$* gene. Heterologous cell expression of wild-type or mutant P2Y$_{12}$ confirmed that the mutation was responsible for the deficiency in P2Y$_{12}$. OSP-1 platelets showed a markedly impaired platelet spreading onto immobilized fibrinogen. Real-time observations of thrombogenesis under a high shear rate (2000 s^{-1}) revealed that thrombi over collagen were small and loosely packed and most of the aggregates were unable to resist against high shear stress in OSP-1. Our data suggest that secretion of endogenous ADP and subsequent P2Y$_{12}$-mediated signaling are critical for platelet aggregation, platelet spreading, and as a consequence, for stabilization of thrombus.

Keywords: $\alpha_{IIb}\beta_3$, initiation codon, mutation, P2Y$_{12}$ deficiency, platelets, thrombogenesis.

Introduction

Platelets play a crucial role not only in a hemostatic plug formation, but also in a pathologic thrombus formation,

Correspondence: Yoshiaki Tomiyama, Department of Hematology and Oncology, Graduate School of Medicine C9, Osaka University, 2-2 Yamadaoka, Suita Osaka 565-0871, Japan.
Tel.: +81 6 6879 3821; fax: +81 6 6879 3879; e-mail: yoshi@hp-blood.med.osaka-u.ac.jp

particularly within atherosclerotic arteries subjected to high shear stress [1,2]. As an initial step in thrombogenesis, platelets adhere to exposed subendothelial matrices such as von Willebrand factor (VWF) and collagen, then become activated and aggregate to each other. These processes are primarily mediated by platelet surface glycoproteins such as GPIb-IX-V, $\alpha_2\beta_1$, GPVI, and $\alpha_{IIb}\beta_3$ (GPIIb-IIIa) [3,4]. In addition, several mediators such as adenosine diphosphate (ADP), thromboxane A$_2$, and thrombin cause further platelet activation and recruitment of circulating platelets to the injury sites through activation of $\alpha_{IIb}\beta_3$ and subsequent binding of VWF and fibrinogen.

Recent studies have demonstrated a critical role for ADP in arterial thrombogenesis [5–7]. ADP is actively secreted from platelet dense granules on platelet activation and is passively released from damaged erythrocytes and endothelial cells. Platelets possess at least two major G protein-coupled ADP receptors that are largely responsible for platelet responses to ADP: P2Y$_1$ and P2Y$_{12}$ [6]. P2Y$_1$ is the G$_q$-coupled receptor responsible for mediating platelet shape change and reversible platelet aggregation through intracellular calcium mobilization [8,9], whereas P2Y$_{12}$ is the G$_i$-coupled receptor responsible for mediating inhibition of adenylyl cyclase and sustained platelet aggregation [10–12]. P2Y$_{12}$ is the therapeutic target of efficacious antithrombotic agents, such as ticlopidine, clopidogrel, and AR-C compounds [5,6], and its congenital deficiency results in a bleeding disorder [13,14]. The analyses of patients with P2Y$_{12}$ deficiency as well as P2Y$_{12}$-null mice would provide more precise information about the role of P2Y$_{12}$ in platelet function than those using P2Y$_{12}$ inhibitors. To date, four different families with a defect in the expression or the function of P2Y$_{12}$ have been characterized [10,13–16]. In this study, we have described a patient with the congenital P2Y$_{12}$ deficiency due to a homozygous mutation in the translation initiation codon and analyzed the role of P2Y$_{12}$ in platelet aggregation, platelet spreading onto immobilized fibrinogen, and thrombogenesis on a type I collagen-coated surface under a high shear rate. Our present data have demonstrated a crucial role of P2Y$_{12}$ in various platelet functions.

Materials and methods

Patient history

The proband (OSP-1) is a 67-year-old Japanese female with a lifelong history of easy bruising. She (OSP-1) was born from non-consanguineous parents who had no hemorrhagic diathesis. Although she showed massive bleeding during delivery of her son, she had no history of transfusions. Patient OSP-1 showed normal platelet count, normal coagulation tests (prothrombin time and activated partial thromboplastin time) and slightly elevated plasma fibrinogen (398 mg dL^{-1}). Ivy bleeding time of the patient was consistently prolonged (> 15 min). Clot retraction by MacFarlane's method was normal (50%; normal values 40%–70%). Her son never suffered from a bleeding tendency. Informed consent for analyzing their platelet function and molecular genetic abnormalities was obtained from OSP-1, her husband and their son.

Preparation of platelet-rich plasma and washed platelet suspension

Platelet-rich plasma (PRP) for aggregation studies was prepared by a centrifugation of whole blood anticoagulated with citrate at 250 *g* for 10 min and then the platelet count was adjusted at 300×10^6 mL^{-1} by platelet-poor plasma. Washed platelets were prepared as previously described [17]. In brief, 6 volumes of freshly drawn venous blood from the patient, her husband, son or healthy volunteers were mixed with 1 volume of acid–citrate–dextrose (ACD; National Institutes of Health Formula A, NIH, Bethesda, MD, USA) and centrifuged at 250 *g* for 10 min to obtain PRP. After incubation with 20 ng mL^{-1} prostaglandin E1 (PGE$_1$; Sigma-Aldrich, St Louis, MO, USA) for 15 min, the PRP was centrifuged at 750 *g* for 10 min, washed three times with 0.05 mol L^{-1} isotonic citrate buffer containing 20 ng mL^{-1} PGE$_1$ and resuspended in an appropriate buffer.

Platelet aggregometry

Platelet aggregation using PRP was monitored by a model PAM-6C platelet aggregometer (Mebanix, Tokyo, Japan) at 37 °C with a stirring rate of 1000 r.p.m. as previously described [18]. Protease-activated receptor 1-activating peptide (PAR1 TRAP, SFLLRNPNDKYEPF) and adenosine 3′,5′-diphosphate (A3P5P) were purchased from Sigma-Aldrich Corp. P2Y$_{12}$ antagonist, AR-C6993MX (2-propylthio-D-fluoromethylene adenosine 5-triphosphate) was a kind gift from AstraZeneca (Loughborough, UK).

Flow cytometry and measurement of intracellular cAMP

Flow cytometric analysis using various monoclonal antibodies (mAbs) specific for platelet membrane glycoproteins was performed as previously described [19].

For measuring intracellular cAMP levels, samples of 200 μL of washed platelets (60×10^6) in Walsh buffer (137 mM of NaCl, 2.7 mM of KCl, 1.0 mM of MgCl$_2$, 3.3 mM of NaH$_2$PO$_4$, 3.8 mM of HEPES, 0.1% of glucose, 0.1% of BSA, pH 7.4) were incubated with 1 μmol L^{-1} PGE$_1$ for 15 min, and then platelets were stimulated with ADP or epinephrine. After incubation for 15 min, total cellular cAMP levels were measured using the Biotrak cAMP enzyme immunoassay system from Amersham Pharmacia Biotech (Piscataway, NJ, USA).

Platelet adhesion assay

Adhesion study was performed as previously described [20]. In brief, non-treated polystyrene 10 cm dishes were coated with 100 μg mL^{-1} human fibrinogen in 5 mL of phosphate-buffered saline (PBS) at 4 °C overnight. After washing with PBS, dishes were blocked with PBS containing 1% of bovine serum albumin (BSA) for 90 min at 37 °C. Aliquots (1 mL) of washed platelets (25×10^6 mL^{-1}) were added to the fibrinogen-coated dishes and incubated at 37 °C. After incubation for 40 min, adherent platelets were fixed with 3.7% formaldehyde, permeabilized with 0.1% Triton X-100 and stained with TRITC-conjugated phalloidin. Platelet morphology and degrees of spreading were determined by fluorescence microscopy (Olympus, Tokyo, Japan).

Platelet thrombus formation under flow conditions

The real-time observation of mural thrombogenesis on a type I collagen-coated surface under a high shear rate (2000 s^{-1}) was performed as previously described [21]. In brief, type I collagen-coated glass coverslips were placed in a parallel plate flow chamber (rectangular type; flow path of 1.9-mm width, 31-mm length, and 0.1-mm height). The chamber was assembled and mounted on a microscope (BX60; Olympus, Tokyo, Japan) equipped with epifluorescent illumination (BX-FLA; Olympus) and a charge-coupled device (CCD) camera system (U-VPT-N; Olympus). Whole blood containing mepacrine-labeled platelets obtained from OSP-1 or control subjects was aspirated through the chamber by a syringe pump (Model CFV-3200, Nihon Kohden, Tokyo, Japan) at a constant flow rate of 0.285 mL min^{-1}, producing a wall shear rate of 2000 s^{-1} at 37 °C.

Amplification and analysis of platelet RNA

Total cellular RNA of platelets was isolated from 20 mL of whole blood, and P2Y$_1$ or P2Y$_{12}$ mRNA was specifically amplified by reverse transcription-polymerase chain reaction (RT-PCR), as previously described [22]. The following primers were constructed based on the published sequence of P2Y$_{12}$ cDNA and used for the first round PCR for P2Y$_{12}$ cDNA: Y12F1, 5′-GGCTGCAATAACTACTACTTACT-GG-3′ [sense, nucleotide(nt) −74 to −50]; Y12R4, 5′-CAGGA-CAGTGTAGAGCAGTGG-3′ (antisense, nt 85 to 105) [10].

Allele-specific restriction enzyme analysis (ASRA)

Genomic DNA was isolated from mononuclear cells using SepaGene kit (Sanko Junyaku Co Ltd, Tokyo, Japan). Amplification of the region around the initiation codon of the $P2Y_{12}$ gene was performed by using primers *Bsr*DI-GF, 5'-CTTTTGTTCTCTAGGTAACCAACAAG̲CAA-3' (sense, the mismatched base is underlined), and Y12R4 (antisense described above) using 250 ng of DNA as a template. These primers can be found in GenBank accession no. AC024886.20 and the sense primer corresponds to 127558–127585. PCR products were then digested with restriction enzyme *Bsr*DI. The resulting fragments were electrophoresed in a 6% polyacrylamide gel.

Construction of P2Y₁₂ expression vectors and cell transfection

The full-length cDNA of wild-type (WT) and mutant $P2Y_{12}$ was amplified by RT-PCR using primers Y12-*Hin*dIII-F, 5'-GAATTCAAGCTTCAAGAAATGCAAGCCGTCGACA-ACCTC-3' (sense, nt −6 -21 for WT, *Eco*RI and *Hin*dIII sites introduced at the 5' end were underlined) or Y12-*Hin*dIII-F2, 5'-GAATTCAAGCTTCAAGAAAGGCAAGCCGTCGAC-AACCTC-3' (sense, nt −6 −21 for mutant), and Y12H-Not-R, 5'-TCTAGAGCGGCCGCTCAATGGTGATGGTGATGA-TGCATTGGAGTCTCTTCATT-3' (antisense, nt 1012–1029, His × 6 were introduced before stop codon, *Not*I and *Xba*I sites introduced at the 5' end were underlined). The amplified fragments were digested with *Hin*dIII and *Not*I, and the resulting 1059-bp fragments (nt −9 −1050) were extracted using QIAquick gel extraction kit (Qiagen, GmbH, Germany). These fragments were inserted into the pcDNA3 (Invitrogen, San Diego, CA, USA) digested with *Hin*dIII and *Not*I. The fragments inserted were characterized by sequence analysis to verify the absence of any other substitutions and the proper insertion of the PCR cartridge into the vector.

A total of 10 μg of WT or mutant $P2Y_{12}$ construct was transfected into human embryonic kidney 293 cells (HEK293 cells, 10^6 cells) using the calcium phosphate method as previously described [22]. Transfectants were lyzed by 1% Triton X-100 PBS containing protease inhibitors 2 days after transfection, and proteins were separated by 7.5% SDS-PAGE. After transferred onto a PVDF membrane, expressed proteins were detected by rabbit anti-His tag antibody.

Results

Platelet aggregation studies

We first examined the expression of platelet membrane glycoproteins in OSP-1 by flow cytometry. The patient's platelets (OSP-1 platelets) normally express GPIb-IX, $\alpha_{IIb}\beta_3$ (GPIIb-IIIa), $\alpha_2\beta_1$, and CD36 (data not shown). Fig. 1 shows platelet aggregation of PRP in response to various agonists. The aggregation of OSP-1 platelets induced by 20 μM of ADP was markedly impaired with only a small and transient
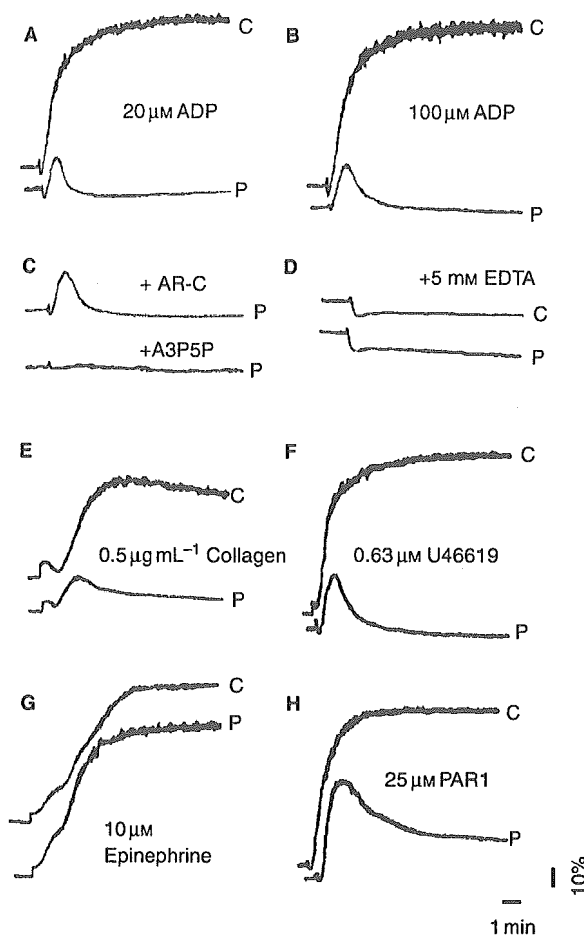
Fig. 1. Platelet aggregation induced by various agonists. Platelet aggregation was induced by various agonists in citrated PRP from patient OSP-1 (labeled 'P') or a control subject (labeled 'C'). Agonists used are (A) 20 μM of ADP, (B) 100 μM of ADP, (C) 20 μM of ADP in the presence of 1 μM of AR-C69931MX ('AR-C'), a specific $P2Y_{12}$-antagonist, or 1 mM of A3P5P ('A3P5P'), a specific $P2Y_1$-antagonist, (D) 20 μM of ADP in the presence of 5 mM of EDTA, (E) 0.5 μg mL^{-1} of collagen, (F) 0.63 μM of U46619, (G) 10 μM of epinephrine, and (H) 25 μM of PAR1-TRAP.

aggregation (Fig. 1A), and the aggregation was still impaired even at 100 μM of ADP (Fig. 1B). As compared with control platelets, the aggregation of OSP-1 platelets was also impaired with a transient aggregation in response to low concentrations of collagen (0.5 μg mL^{-1}, Fig. 1E), U46619 (0.63 μM, Fig. 1F), or PAR1 TRAP (25 μM, Fig. 1H). In response to 1.3 mg mL^{-1} ristocetin (not shown) or 10 μM of epinephrine (Fig. 1G), OSP-1 platelets aggregated normally. When OSP-1 platelets were stimulated with 20 μM of ADP in the presence of 5 mM of EDTA, the light transmission decreased equivalent to control platelets suggesting that OSP-1 platelets changed shape normally (Fig. 1D). We then examined effects of ADP receptor antagonists on the aggregation of OSP-1 platelets induced by 20 μM of ADP. A total of 1 mM of A3P5P, a specific $P2Y_1$ antagonist, abolished the residual response of OSP-1 platelets to ADP, whereas 1 μM of AR-C69931MX, a specific $P2Y_{12}$
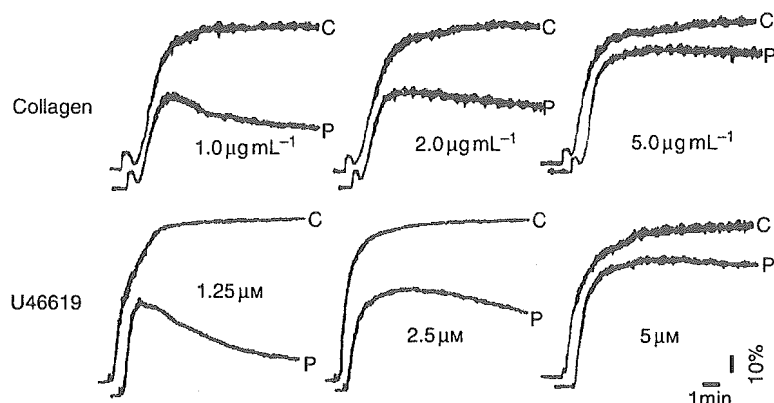
Fig. 2. Platelet aggragation induced by collagen or U46619 at various concentrations. Platelet aggregation in citrated PRP from patient OSP-1 (labeled 'P') or a control subject (labeled 'C') was induced by various concentrations of collagen or U46619. At high concentrations of collagen or U46619, OSP-1 platelets aggregate almost normally.

antagonist, did not induce an additional inhibition on the platelet aggregation (Fig. 1C). These data suggest that the impaired response of the patient's platelets may be due to an abnormality in signaling evoked by ADP and that $P2Y_{12}$-mediated signaling rather than $P2Y_1$-mediated signaling may be completely defective in patient OSP-1.

We also examined the aggregation of OSP-1 platelets induced by higher concentrations of agonists. As shown in Fig. 2, the aggregation response of OSP-1 platelets improved as the concentrations of agonists increased, and they aggregated almost normally in response to high concentrations of collagen (5 μg mL^{-1}), U46619 (5 μM), or PAR1 TRAP (100 μM) (not shown). In addition, we confirmed that 1 μM of AR-C69931MX conferred essentially the same defect on the aggregation of control platelets in response to U46619 as that of OSP-1 platelets and did not further inhibit OSP-1 platelet aggregation induced by 5 μg mL^{-1} of collagen, 5 μM of U46619, or 100 μM of PAR1 TRAP (data not shown). These data indicated that at high concentrations of agonists OSP-1 platelets showed the specifically impaired aggregation to ADP.

Effect of ADP on PGE_1-stimulated cAMP accumulation in platelets

To determine whether $P2Y_{12}$-mediated signaling is specifically impaired, we examined an inhibitory effect of ADP on 1 μM of PGE_1-stimulated cAMP accumulation in platelets from the patient, her husband, their son, and healthy unrelated controls. ADP inhibited intracellular cAMP levels in platelets from the patient's husband, son and healthy unrelated controls (not shown) by approximately 80%, whereas the inhibition was only 15% in the patient's platelets (Fig. 3). In contrast to ADP, epinephrine normally inhibited cAMP accumulation in platelets from the patient as well as her husband and son. These results strongly suggest that the defect could be due to an abnormality in G_i coupling ADP receptor, $P2Y_{12}$.
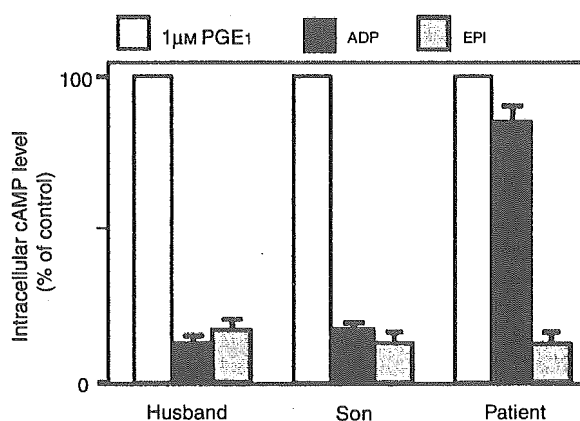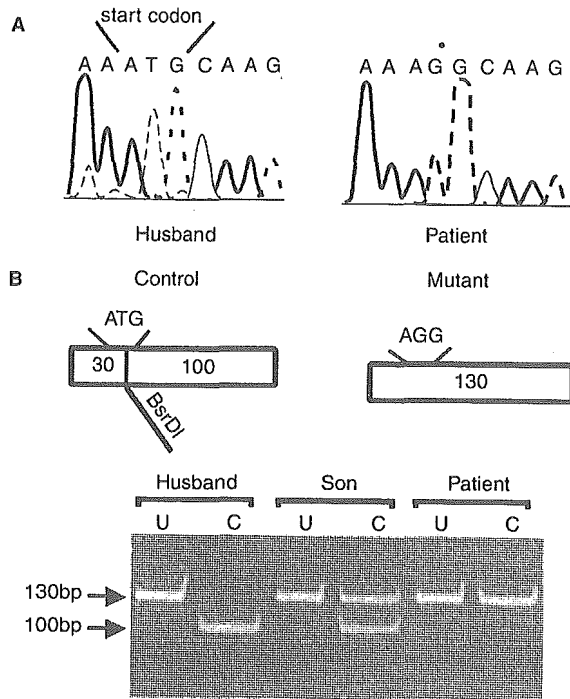

Fig. 3. Effect of ADP or epinephrine on the inhibition of PGE_1-induced cAMP accumulation in platelets. Washed platelets from patient OSP-1, husband or son were incubated with 1 μM of PGE_1 for 15 min and stimulated with 20 μM of ADP or 10 μM of epinephrine. Intracellular cAMP levels were expressed as a percent of cAMP levels in the absence of agonists. Results in OSP-1 are the mean of two experiments.

Nucleotide sequence analysis of cDNA and genomic DNA of $P2Y_{12}$

To reveal a molecular genetic defect in OSP-1, we analyzed the entire coding regions of both $P2Y_1$ and $P2Y_{12}$ cDNAs amplified from platelet mRNA by RT-PCR. A single nucleotide substitution (T → G) was identified within the translation initiation codon (A**T**G → A**G**G) in the patient's $P2Y_{12}$ cDNA (Fig. 4A). This substitution was also confirmed by reverse sequencing. No other nucleotide substitutions were detected within the coding region of either $P2Y_{12}$ or $P2Y_1$ cDNA from the patient. OSP-1 appeared homozygous for the substitution, and the substitution was not detected in 20 control subjects.

Nucleotide sequence analysis of PCR fragments from the patient's genomic DNA also suggested the homozygosity of the substitution (data not shown). To further confirm the homo-
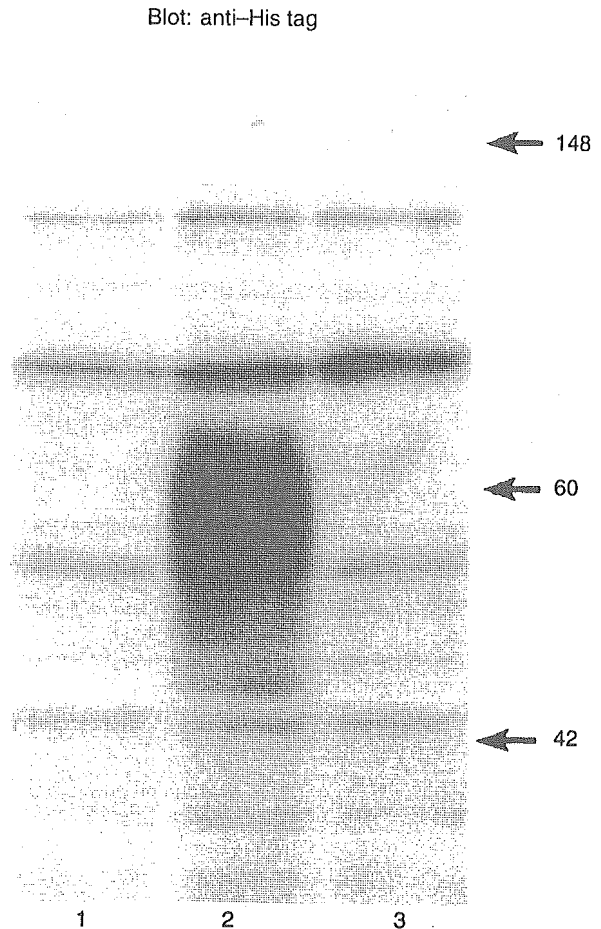
© 2005 International Society on Thrombosis and Haemostasis

A

start codon

A A A T G C A A G   A A A G G C A A G

Husband   Patient

B   Control   Mutant

ATG   AGG

| 30 | 100 | | 130 |

*Bsr*DI

Husband   Son   Patient

U C   U C   U C

130bp →

100bp →

Fig. 4. Sequence analysis of P2Y$_{12}$ cDNA and restriction enzyme analysis of the P2Y$_{12}$ gene. (A) cDNA obtained by RT-PCR from platelet mRNA was analyzed by sequencing using a sense primer Y12F1. (B) PCR was performed to generate 130-bp fragments including initiation codon of P2Y$_{12}$ as described in Materials and methods. Undigested (U) or digested (C) PCR products with *Bsr*DI were analyzed on a 6% polyacrylamide gel. In patient OSP-1, the T → G mutation at position 2 abolishes a *Bsr*DI restriction site.

Blot: anti–His tag

← 148

← 60

← 42

1   2   3

Fig. 5. Expression of P2Y$_{12}$ in HEK293 cells transfected with WT or mutant His-tag attached P2Y$_{12}$. Wild-type or mutant P2Y$_{12}$ construct was transfected into HEK293 cells using the calcium phosphate method. Transfectants were lyzed by 1% Triton X-100 PBS containing protease inhibitors 2 days after transfection. Cell lysates from mock transfectant (lane 1), cells transfected with WT P2Y$_{12}$ (lane 2) or mutant P2Y$_{12}$ (lane 3) were separated by 7.5% SDS-PAGE, and immunoblot was performed by anti-His-tag antibodies.

zygosity, allele-specific restriction enzyme analysis (ASRA) was performed. The region around the initiation codon of the P2Y$_{12}$ gene was amplified by PCR using primers *Bsr*DI-GF and Y12R4. A restriction site for *Bsr*DI would be abolished by the T → G substitution. As shown in Fig. 4B, ASRA clearly indicated that the patient and her son were homozygous and heterozygous for the substitution, respectively. These results also confirm that the substitution is inheritable.

Heterologous cell expression of WT and mutant P2Y$_{12}$

As the substitution at the translation initiation codon might induce an alternative translation starting at downstream ATGs leading to an expression of shorter form of P2Y$_{12}$, we decided to investigate effects of the substitution found in the patient on the expression of P2Y$_{12}$. Expression vectors encoding WT and mutant P2Y$_{12}$ in which His-tag was attached at the C-terminal portion of P2Y$_{12}$ were constructed as described in the Materials and methods. Wild-type or mutant P2Y$_{12}$ construct was transfected into HEK 293 cells, and then expressed proteins were analyzed 48 h after transfection in an immunoblot assay employing anti-His antibodies. As shown in Fig. 5, WT P2Y$_{12}$ protein with an apparent molecular weight of ∼60 KDa was expressed in 293 cells as a His-tag-positive protein. In sharp

contrast, the mutant P2Y$_{12}$-expression vector failed to express any His-tag-positive protein. These results provide strong evidence that the T → G substitution at the translation initiation codon of P2Y$_{12}$ cDNA is responsible for the P2Y$_{12}$ deficiency.

Platelet spreading on immobilized fibrinogen

As it has been well documented that release of endogenous ADP is required for full platelet spreading onto immobilized fibrinogen [23], we next analyzed the patient's platelet spreading in order to evaluate the role of P2Y$_{12}$. Control platelets adhered to fibrinogen underwent morphological changes ranging from filopodia protrusion to complete spreading, and 50.5% ± 21.3% of the adherent platelets spread ($n = 3$) (Fig. 6A). In sharp contrast, the patient's platelets showed an
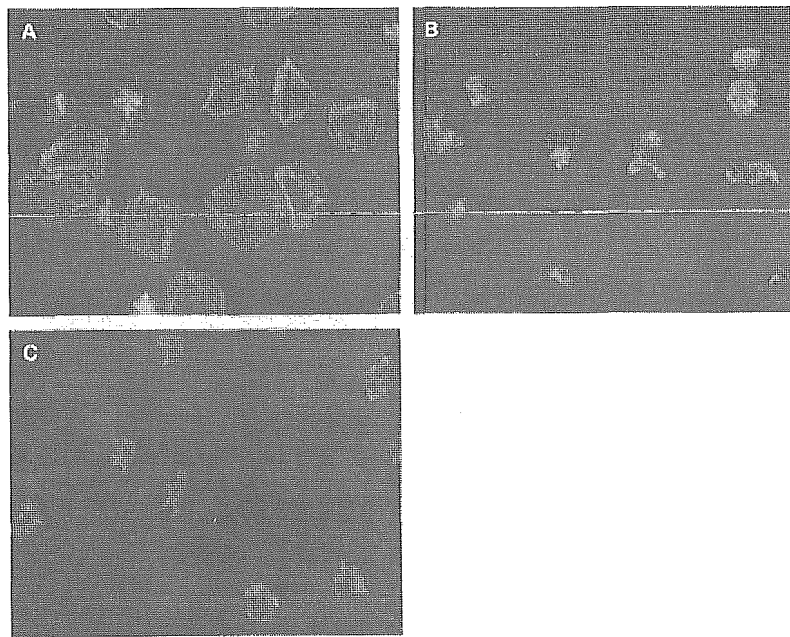
Fig. 6. Platelet spreading on immobilized fibrinogen. (A,B) Washed platelets from a control subject were applied onto fibrinogen-coated polystyrene dishes and incubated at 37 °C for 40 min without any inhibitor (A) or with 1 μM of AR-C69931MX (B). (C) Washed platelets from the patient were applied onto fibrinogen-coated polystyrene dishes and incubated at 37 °C for 40 min without any inhibitor. Adherent platelets were then fixed, permeabilized and stained with TRITC-conjugated phalloidin. Platelet morphology was analyzed by fluorescence microscopy.

impaired spreading and only 2.3% ± 1.4% of the adherent platelets spread ($n = 3$, $P < 0.001$, Fig. 6C). Similar results were obtained with control platelets in the presence of 1 μM of AR-C69931MX (6.2% ± 2.2%, $n = 3$, $P < 0.001$, Fig. 6B). In addition, 1 mM of A3P5P also markedly inhibited platelet spreading ($n = 3$, 10.1% ± 2.2%, $P < 0.001$, not shown). These results suggest that both $P2Y_{12}$ and $P2Y_1$ are necessary for platelet spreading.

Platelet-thrombus formation on immobilized collagen under flow conditions

To investigate the role of $P2Y_{12}$ in thrombus formation, we observed the real-time process of mural thrombogenesis on a type I collagen-coated surface under flow conditions with high shear rate ($2000\ s^{-1}$) using the whole blood from OSP-1. Real-time observation revealed that thrombi formed on type I collagen were unstable. As platelet aggregates of the patient were loosely packed each other and unable to resist against high shear stress, most of the aggregates at the apex of the thrombi came off the thrombi constantly. On the other hand, most of thrombi formed by control platelets were densely packed with higher fluorescent intensity and were stable with constant growth during observation (Video 1 and 2).

As shown in Fig. 7A, the area covered with patient platelets after 7 min of flow was greater than that of control platelets (91.8% ± 0.3% vs. 82.2% ± 1.4%, $n = 3$, $P < 0.01$). However, thrombi formed by OSP-1 platelets were loosely packed, whereas thrombi were large and densely packed in controls. The overall fluorescent intensity of thrombi of OSP-1 platelets

was lower than that of control platelets. Three-dimensional analysis revealed the striking difference in size and shape of individual thrombus formed after 10 min between the patient and control platelets (Fig. 7B). Thrombi formed by control platelets were large in size, clearly edged and surrounded by thrombus-free areas. On the other hand, individual thrombus formed by patient platelets was mostly small and appeared to be a thin layer of platelet aggregates. Thrombus height at the plateau phase was 10.2 ± 0.4 μm, which was less than half of controls (21.2 ± 0.4 μm).

Discussion

$P2Y_{12}$ coupled with $G\alpha_i$, primarily with $G\alpha_{i2}$, consists of 342 amino acid residues with seven transmembrane domains (TM), and its deficiency is responsible for congenital bleeding diathesis [10–16]. To date, five mutations responsible for a defect in the expression or the function of $P2Y_{12}$ in four different families have been demonstrated [10,15,16]. Patient ML possessed a mutation consisting of a two nucleotide deletion at amino acid 240 (near the N-terminal end of TM6), which would lead to a premature termination of $P2Y_{12}$ [10,14]. A two nucleotide deletions at amino acid 98 (next to the N-terminal end of TM3) and a single nucleotide deletion occurring just beyond TM3 were identified in other two families, both of which would lead to a premature termination of $P2Y_{12}$ [13,15]. However, in these reports expression studies had not been performed to show the direct association between these mutations and the $P2Y_{12}$ deficiency [10,15]. Patient AC, whose platelets expressed dysfunctional $P2Y_{12}$ with normal

A

| 1 min | 3 min | 5 min | 7 min |

Control

Patient
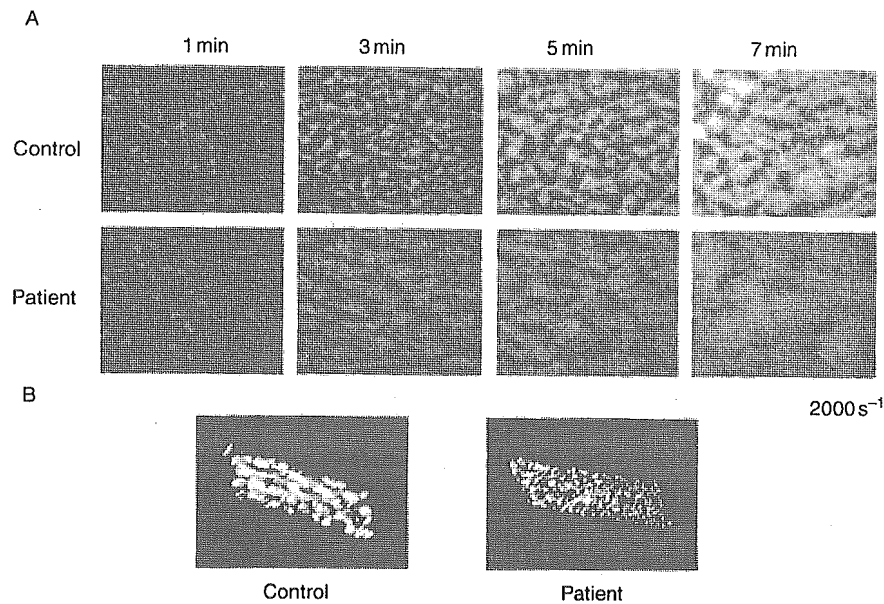
B

2000 s^{-1}

Control   Patient

Fig. 7. Thrombus formation on immobilized collagen under flow conditions. (A) Whole blood containing mepacrine-labeled platelets obtained from the patient or control subjects was aspirated through a chamber with type 1 collagen-coated coverslips. Thrombi formed under a high shear rate (2000 s^{-1}) at indicated time points were observed using a microscope equipped with epifluorescent illumination and a CCD camera system. (B) Three-dimensional structure of thrombi formed after 10 min flow by platelets from the patient or a control subject was analyzed.

binding capacity of 2-methylthioadenosine 5'-diphosphate (2MeS-ADP), was compound heterozygous for Arg256 → Gln in TM6 and for Arg265 → Trp in the third extracellular loop of P2Y$_{12}$. Platelets from patient AC showed an increased platelet aggregation at high dose ADP compared with low dose ADP, suggesting the presence of residual receptor function [16]. In this study, we described a patient (OSP-1) with congenital bleeding diathesis bearing a novel homozygous mutation within the translation initiation codon (A̱TG → A̱GG) of the P2Y$_{12}$ gene. Consistent with previous studies, the aggregation of OSP-1 platelets with P2Y$_{12}$ deficiency was impaired to various agonists such as collagen, U46619, and PAR1 TRAP at low concentrations, but almost normal at high concentrations [11–14]. These findings confirmed the critical role of P2Y$_{12}$-mediated signaling evoked by endogenous ADP in platelet aggregation induced by low concentrations of agonists. In contrast to patient AC with residual P2Y$_{12}$-mediated signaling, the impaired platelet aggregation in OSP-1 in response to ADP was neither improved even at 100 μM of ADP stimulation nor reduced by adding 1 μM of AR-C69931MX, suggesting a complete loss of the P2Y$_{12}$ function. Family study confirmed that patient OSP-1 was homozygous for the mutation, and our expression study demonstrated that the mutation is responsible for the P2Y$_{12}$ deficiency.

A number of examples of mutations in the translation initiation codons have been demonstrated in various diseases [24]. Although some cases having mutations in the initiation codons did not express any related abnormal protein, Pattern *et al.* showed an abnormal Gα$_s$ protein possibly synthesized as a result of initiation at downstream ATGs due to a mutation at an initiation codon (A̱TG → G̱TG) in patients with

Albright's hereditary osteodystrophy [24,25]. In OSP-1, we detected the T → G mutation at position +2, and our expression study denied the possibility that the substitution might induce an alternative translation at downstream ATGs leading to an expression of shorter form of P2Y$_{12}$.

As to platelet spreading onto immobilized fibrinogen, OSP-1 platelets showed the impaired platelet spreading. Similarly, A3P5P inhibited the platelet spreading. It has been well documented that release of endogenous ADP is required for full platelet spreading onto immobilized fibrinogen [23], and Obergfell *et al.* [26] have demonstrated that the platelet spreading requires sequential activation of Src and Syk in proximately to α$_{IIb}$β$_3$. In contrast to the ADP-induced platelet shape change shown in OSP-1 platelets in the platelet aggregometer, our data indicated that both P2Y$_{12}$ and P2Y$_1$ were necessary for the full spreading onto immobilized fibrinogen.

Employing clopidogrel or AR-C69931 MX as an inhibitor for P2Y$_{12}$, several studies examined the role of P2Y$_{12}$ in thrombogenesis under flow conditions [27–30]. However, some discrepancy between the studies was pointed out and non-specific effects of these inhibitors were not completely ruled out [28–30]. As patient OSP-1 was deficient in P2Y$_{12}$ as shown in this study, it would be informative to examine the real-time process of thrombogenesis on a type I collagen-coated surface under a high shear rate (2000 s^{-1}) employing whole blood obtained from OSP-1. Our data demonstrated that P2Y$_{12}$-deficiency led to the loosely packed thrombus and the impaired thrombus growth with enhancing adhesion to collagen, which was consistent with the study by Remijn *et al.* [30] employing patient ML's platelets. The increase in platelet adhesion to

collagen was probably due to the impaired platelet consumption by the growing thrombi [27,30]. Moreover, our real-time observation indicated that the loosely packed aggregates were unable to resist against high shear stress, and then most of the aggregates at the apex of the thrombi came off the thrombi. In contrast, Andre *et al.* [12] did not detect significant differences in *ex vivo* thrombus volume formed over human type III collagen under a shear rate of 871 s^{-1} between P2Y$_{12}^{-/-}$ and WT mice. Although Andre *et al.* used non-anticoagulated mouse blood instead of anticoagulated blood, Roald *et al.* [27] demonstrated that clopidogrel significantly reduced the thrombus volume over type III collagen employing non-anticoagulated human blood. Loosely packed platelet thrombi with swollen non-degranulated platelets were detected following clopidogrel intake, whereas densely packed thrombi with partly fused platelets were detected before clopidogrel intake by electron microscopy [27]. Thus, it is likely that differences between human and mouse, rather than those between non-anticoagulated and anticoagulated blood, may account for the discrepancy. Nevertheless, they showed that *ex vivo* thrombi were loosely packed and that only small and unstable thrombi were formed in P2Y$_{12}^{-/-}$ mice without reaching occlusive size in mesenteric artery injury model *in vivo* [12].

Our present study has demonstrated the novel mutation responsible for the P2Y$_{12}$ deficiency and suggested that secretion of endogenous ADP and subsequent P2Y$_{12}$-mediated signaling is critical for platelet aggregation, platelet spreading, and as a consequence, for stabilization of thrombus. Mild bleeding tendency observed in patient OSP-1 further emphasizes the efficacy of P2Y$_{12}$ receptor as a therapeutic target for thrombosis.

Acknowledgements

Supplementary material

The following supplementary material is available online at http://www.blackwell-synergy.com/loi/jth:

Figure S1. Perfusion study using control platelets. A real-time movie of platelets perfused over type-I collagen shows that thrombi formed by control platelets are densely packed and stable. This 5-second movie was taken at 5-minute perfusion under a high shear rate (2000 s^{-1}).

Figure S2. Perfusion study using OSP-1 platelets. A real-time movie of platelets perfused over type-I collagen shows that thrombi formed by the patient OSP-1 platelets are loosely packed and unstable. Newly formed aggregates on the top of thrombi keep on moving toward downstream and some aggregates came off the thrombi. This 5-second movie was taken at 5-minute perfusion under a high shear rate (2000 s^{-1}).

References

1 Fuster V, Badimon L, Badimon JJ, Chesebro JH. The pathogenesis of coronary artery disease and the acute coronary syndromes. *N Engl J Med* 1992; **326**: 242–50.

2 Antithrombotic Trialists' Collaboration. Collaborative meta-analysis of randomised trials of antiplatelet therapy for prevention of death, myocardial infarction, and stroke in high risk patients. *BMJ* 2002; **324**: 71–86.

3 Savage B, Almus-Jacobs F, Ruggeri ZM. Specific synergy of multiple substrate–receptor interactions in platelet thrombus formation under flow. *Cell* 1998; **94**: 657–66.

4 Tomiyama Y, Shiraga M, Shattil SJ. Platelet Membrane Proteins as Adhesion Receptors. In: Gresele P, Page C, Fuster V, Vermylen J, eds. *Platelets in thrombotic and non-thrombotic disorders pathophysiology, pharmacology and therapeutics.* Cambridge, UK: Cambridge, 2002: 80–92.

5 CAPRIE Steering Committee. A randomised, blinded, trial of clopidogrel versus aspirin in patients at risk of ischaemic events (CAPRIE). *Lancet* 1996; **348**: 1329–39.

6 Gachet C. ADP receptors of platelets and their inhibition. *Thromb Haemost* 2001; **86**: 222–32.

7 Dorsam RT, Kunapuli SP. Central role of the P2Y$_{12}$ receptor in platelet activation. *J Clin Invest* 2004; **113**: 340–5.

8 Fabre JE, Nguyen M, Latour A, Keifer JA, Audoly LP, Coffman TM, Koller BH. Decreased platelet aggregation, increased bleeding time and resistance to thromboembolism in P2Y$_1$-deficient mice. *Nat Med* 1999; **5**: 1199–202.

9 Leon C, Hechler B, Freund M, Eckly A, Vial C, Ohlmann P, Dierich A, LeMeur M, Cazenave JP, Gachet C. Defective platelet aggregation and increased resistance to thrombosis in purinergic P2Y$_1$ receptor-null mice. *J Clin Invest* 1999; **104**: 1731–7.

10 Hollopeter G, Jantzen HM, Vincent D, Li G, England L, Ramakrishnan V, Yang RB, Nurden A, Julius D, Conley PB. Identification of the platelet ADP receptor targeted by antithrombotic drugs. *Nature* 2001; **409**: 202–7.

11 Foster CJ, Prosser DM, Agans JM, Zhai Y, Smith MD, Lachowicz JE, Zhang FL, Gustafson E, Monsma Jr FJ, Wiekowski MT, Abbondanzo SJ, Cook DN, Bayne ML, Lira SA, Chintala MS. Molecular identification and characterization of the platelet ADP receptor targeted by thienopyridine antithrombotic drugs. *J Clin Invest* 2001; **107**: 1591–8.

12 Andre P, Delaney SM, LaRocca T, Vincent D, DeGuzman F, Jurek M, Koller B, Phillips DR, Conley PB. P2Y$_{12}$ regulates platelet adhesion/activation, thrombus growth, and thrombus stability in injured arteries. *J Clin Invest* 2003; **112**: 398–406.

13 Cattaneo M, Lecchi A, Randi AM, McGregor JL, Mannucci PM. Identification of a new congenital defect of platelet function characterized by severe impairment of platelet responses to adenosine diphosphate. *Blood* 1992; **80**: 2787–96.

14 Nurden P, Savi P, Heilmann E, Bihour C, Herbert JM, Maffran JP, Nurden A. An inherited bleeding disorder linked to a defective interaction between ADP and its receptor on platelets. Its influence on glycoprotein IIb-IIIa complex function. *J Clin Invest* 1995; **95**: 1612–22.

15 Conley P, Jurek M, Vincent D, Lecchi A, Cattaneo M. Unique mutations in the P2Y$_{12}$ locus of patients with previously described defects in ADP-dependent aggregation [abstract]. *Blood* 2001; **98**: 43b. Abstract 3778.

16 Cattaneo M, Zighetti ML, Lombardi R, Martinez C, Lecchi A, Conley PB, Ware J, Ruggeri ZM. Molecular bases of defective signal transduction in the platelet P2Y$_{12}$ receptor of a patient with congenital bleeding. *Proc Natl Acad Sci USA* 2003; **100**: 1978–83.

17 Shiraga M, Tomiyama Y, Honda S, Suzuki H, Kosugi S, Tadokoro S, Kanakura Y, Tanoue K, Kurata Y, Matsuzawa Y. Involvement of Na$^+$/Ca^{2+} exchanger in inside-out signaling through the platelet integrin $\alpha_{IIb}\beta_3$. *Blood* 1998; **92**: 3710–20.

18 Tomiyama Y, Tsubakio T, Piotrowicz RS, Kurata Y, Loftus JC, Kunicki TJ. The Arg-Gly-Asp (RGD) recognition site of platelet glycoprotein IIb-IIIa on nonactivated platelets is accessible to high-affinity macromolecules. *Blood* 1992; **79**: 2303–12.

19 Honda S, Tomiyama Y, Aoki T, Shiraga M, Kurata Y, Seki J, Matsuzawa Y. Association between ligand-induced conformational changes of integrin $\alpha_{IIb}\beta_3$ and $\alpha_{IIb}\beta_3$-mediated intracellular Ca^{2+} signaling. *Blood* 1998; **92**: 3675–83.

20 Kato H, Honda S, Yoshida H, Kashiwagi H, Shiraga M, Honma N, Kurata K, Tomiyama Y. SHPS-1 negatively regulates integrin $\alpha_{IIb}\beta_3$ function through CD47 without disturbing FAK phosphorylation. *J Thromb Haemost* 2005; **3**: 763–74.

21 Tsuji S, Sugimoto M, Miyata S, Kuwahara M, Kinoshita S, Yoshioka A. Real-time analysis of mural thrombus formation in various platelet aggregation disorders: distinct shear-dependent roles of platelet receptors and adhesive proteins under flow. *Blood* 1999; **94**: 968–75.

22 Honda S, Tomiyama Y, Shiraga M, Tadokoro S, Takamatsu J, Saito H, Kurata Y, Matsuzawa Y. A two-amino acid insertion in the Cys146-Cys167 loop of the α_{IIb} subunit is associated with a variant of Glanzmann thrombasthenia. Critical role of Asp163 in ligand binding. *J Clin Invest* 1998; **102**: 1183–92.

23 Haimovich B, Lipfert L, Brugge JS, Shattil SJ. Tyrosine phosphorylation and cytoskeletal reorganization in platelets are triggered by interaction of integrin receptors with their immobilized ligands. *J Biol Chem* 1993; **268**: 15868–77.

24 Cooper D. Human gene mutations affecting RNA processing and translation. *Ann Med* 1993; **25**: 11–7.

25 Patten J, Johns D, Valle D, Eil C, Gruppuso PA, Steele G, Smallwood PM, Levine MA. Mutation in the gene encoding the stimulatory G protein of adenylate cyclase in Albright's hereditary osteodystrophy. *N Engl J Med* 1990; **322**: 1412–9.

26 Obergfell A, Eto K, Mocsai A, Buensuceso C, Moores SL, Brugge JS, Lowell CA, Shattil SJ. Coordinate interactions of Csk, Src, and Syk kinases with $\alpha IIb\beta 3$ initiate integrin signaling to the cytoskeleton. *J Cell Biol* 2002; **157**: 265–75.

27 Roald HE, Barstad RM, Kierulf P, Skjorten F, Dickinson JP, Kieffer G, Sakariassen KS. Clopidogrel - a platelet inhibitor which inhibits thrombogenesis in non-anticoagulated human blood independently of the blood flow conditions. *Thromb Haemost* 1994; **71**: 655–62.

28 Turner NA, Moake JL, McIntire LV. Blockade of adenosine diphosphate receptors P2Y$_{12}$ and P2Y$_1$ is required to inhibit platelet aggregation in whole blood under flow. *Blood* 2001; **98**: 3340–5.

29 Goto S, Tamura N, Handa S. Effects of adenosine 5'-diphosphate (ADP) receptor blockade on platelet aggregation under flow. *Blood* 2002; **99**: 4644–5.

30 Remijn JA, Wu YP, Jeninga EH, IJsseldiik MJ, van Willigen G, de Groot PG, Sixma JJ, Nurden AT, Nurden P. Role of ADP receptor P2Y$_{12}$ in platelet adhesion and thrombus formation in flowing blood. *Arterioscler Thromb Vasc Biol* 2002; **22**: 686–91.